

Computation of Incompressible Navier-Stokes Equations by Local RBF-based Differential Quadrature Method

C. Shu^{1,2}, H. Ding², K.S. Yeo²

Abstract: Local radial basis function-based differential quadrature (RBF-DQ) method was recently proposed by us. The method is a natural mesh-free approach. It can be regarded as a combination of the conventional differential quadrature (DQ) method with the radial basis functions (RBFs) by means of taking the RBFs as the trial functions in the DQ scheme. With the computed weighting coefficients, the method works in a very similar fashion as conventional finite difference schemes. In this paper, we mainly concentrate on the applications of the method to incompressible flows in the steady and unsteady regions. The multiquadric (MQ) radial basis functions are chosen in this study for their exponential convergence. Three two-dimensional cases are tested, and they are the driven-cavity flow, flow past one isolated cylinder at moderate Re number, and flow around two staggered circular cylinders. Excellent numerical results are obtained. The success of these numerical simulations indicates the flexibility and good performance of the method in simulating incompressible flow with geometrical and dynamic complexity.

keyword: mesh-free, meshless, radial basis function, differential quadrature, incompressible flow, staggered cylinders

1 Introduction

The differential quadrature (DQ) method was introduced by Richard Bellman and his associates in the early of 1970's [Bellman, Kashef, and Casti (1972)], following the idea of integral quadrature. The basic idea of the DQ method is that any derivative at a mesh point can be approximated by a weighted linear sum of all the functional values along a mesh line. The key procedure in the DQ method is the determination of weighting coef-

ficients. As shown by [Shu and Richards (1992)], when the solution of a partial differential equation (PDE) is approximated by a high order polynomial, the weighting coefficients can be computed by a simple algebraic formulation or by a recurrence relationship. The details of the DQ method can be found in the book of [Shu (2000)]. On the other hand, it is noted that the polynomial approximation in the DQ method is along a straight line. This means that numerical discretization of derivatives by the DQ method is also along a straight line. Due to this feature, the DQ method cannot be directly applied to irregular domain problems. "Truly" meshless property is another important consideration. It is well-known that meshless local Petrov-Galerkin method (MLPG) [Lin and Atluri (2001), Atluri and Shen (2002), Atluri, Han, and Rajendran (2004), Atluri (2004)], which is based the moving least-square technique, is a "truly" meshless approach. This means that its discretization process does not involve any mesh. As will be shown in this paper, the combination of radial basis functions (RBFs) and DQ technique is another naturally meshless approach.

Initially, RBFs were developed for multivariate data and function interpolation. However, their "truly" mesh-free nature motivated researchers to use them to deal with partial differential equations. The first trial of such exploration was made by [Kansa (1990)]. Subsequently, [Forberg and Driscoll (2002)], [Hon and Wu (2000)], [Chen, Brebbia, and Power (1998)], [Fasshauer (1997)], [Chen and Tanaka (2002)], [Mai-Duy and Tran-Cong (2001a, 2001b)] also made great contributions in this development. It should be noted that most of above works related to the application of RBFs for the numerical solution of PDEs are actually based on the function approximation instead of derivative approximation. In other words, these works directly substitute the expression of function approximation by RBFs into a PDE, and then change the dependent variables into the coefficients of function approximation. The process is very complicated, especially

¹ Corresponding author, Email: mpeshuc@nus.edu.sg.

² Department of Mechanical Engineering, National University of Singapore, Singapore 119260.

for non-linear problems. To remove this difficulty, [Wu and Shu (2002)], [Shu, Ding, and Yeo (2003)] developed the RBF-based differential quadrature (RBF-DQ) method. The RBF-DQ method directly approximates derivatives of a PDE, which combines the mesh-free nature of RBFs with the derivative approximation of differential quadrature (DQ) method. In the local MQ-DQ approach, any spatial derivative at a knot is approximated by a linear weighted sum of all the functional values in the local supporting region around the reference knot. The weighting coefficients in the derivative approximation are determined by MQ approximation of the function and linear vector space analysis. Recently, [Tolstykh and Shirobokov (2003)] also proposed a RBFs-based derivative approximation scheme, in which an approximate formula for the derivative discretization is constructed based on the local RBF-interpolants. Due to the similarity between the local supports and the stencils in finite difference methods, the approach is regarded as using radial basis functions in a “finite difference mode”. This approach is very similar to the local RBF-DQ method. The main difference between the two methods is that the local RBF-DQ formulations are derived from the concept of differential quadrature while the approach of [Tolstykh and Shirobokov (2003)] is constructed from the idea of finite difference schemes.

In general, the local RBF-DQ method is very flexible, and simple in code writing, and it can be consistently well applied to linear and nonlinear problems. Moreover, the problem of ill-conditioned global matrix in the RBF-based scheme is completely avoided in this method. Thus, it can employ a large number of nodes to solve a practical problem without the requirement of careful preconditioning. Some fundamental issues of this method are shown in [Shu, Ding, and Yeo (2003)]. This paper mainly focuses on the applicability of local MQ-DQ method for simulation of two-dimensional incompressible viscous flows with geometrical and dynamic complexity.

2 Local MQ-DQ Method

The details and fundamental issues of local MQ-DQ method have been shown in [Shu, Ding, and Yeo (2003)]. Some basic formulations for derivative approximation will be shown below. Following the work of [Shu, Ding, and Yeo (2003)], the n th order derivative of a smooth function $f(x, y)$ with respect to x , $f_x^{(n)}$, and its m th or-

der derivative with respect to y , $f_y^{(m)}$, at (x_i, y_i) can be approximated by local MQ-DQ method as

$$f_x^{(n)}(x_i, y_i) = \sum_{k=1}^N w_{i,k}^{(n)} f(x_k, y_k) \quad (1)$$

$$f_y^{(m)}(x_i, y_i) = \sum_{k=1}^N \bar{w}_{i,k}^{(m)} f(x_k, y_k) \quad (2)$$

where N is the number of knots used in the supporting region, $w_{i,k}^{(n)}, \bar{w}_{i,k}^{(m)}$ are the DQ weighting coefficients in the x and y directions. The determination of weighting coefficients is based on the analysis of function approximation and the analysis of linear vector space.

In the local MQ-DQ method, MQ approximation is only applied locally. At any knot, there is a supporting region represented by a square, in which there are N knots randomly distributed. The function in this region can be locally approximated by MQ RBFs as

$$f(x, y) = \sum_{j=1, j \neq i}^N \lambda_j g_j(x, y) + \lambda_i \quad (3)$$

where λ_j is a constant, and

$$g_j(x, y) = \sqrt{(x - x_j)^2 + (y - y_j)^2 + c_j^2} \\ - \sqrt{(x - x_i)^2 + (y - y_i)^2 + c_i^2} \quad (4)$$

c_j is the shape parameter to be given by the user.

It is easy to see that $f(x, y)$ in equation (3) constitutes a N -dimensional linear vector space \mathbf{V}^N with respect to the operation of addition and multiplication. From the concept of linear independence, the bases of a vector space can be considered as linearly independent subset that spans the entire space. In the space \mathbf{V}^N , one set of base vectors is $g_i(x, y) = 1$, and $g_j(x, y), j = 1, \dots, N$ but $j \neq i$ given by equation (4). From the property of a linear vector space, if all the base functions satisfy the linear equation (1) or (2), so does any function in the space \mathbf{V}^N represented by equation (3). There is an interesting feature. From equation (3), while all the base functions are given, the function $f(x, y)$ is still unknown since the coefficients λ_i are unknown. However, when all the base functions satisfy equation (1) or (2), we can guarantee that $f(x, y)$ also satisfies equation (1) or (2). In

other words, we can guarantee that the solution of a partial differential equation approximated by local MQ satisfies equation (1) or (2). Thus, when the weighting coefficients of DQ approximation are determined by all the base functions, they can be used to discretize the derivatives in a partial differential equation. That is the essence of the MQ-DQ method.

Following the work of [Shu, Ding, and Yeo (2003)], the weighting coefficient matrix of the x -derivative can be determined by

$$[G][W^n]^T = \{G_x\} \quad (5)$$

where $[W^n]^T$ is the transpose of the weighting coefficient matrix $[W^n]$, and

$$\begin{aligned} [W^n] &= \begin{bmatrix} w_{1,1}^{(n)} & w_{1,2}^{(n)} & \cdots & w_{1,N}^{(n)} \\ w_{2,1}^{(n)} & w_{2,2}^{(n)} & \cdots & w_{2,N}^{(n)} \\ \vdots & \vdots & \ddots & \vdots \\ w_{N,1}^{(n)} & w_{N,2}^{(n)} & \cdots & w_{N,N}^{(n)} \end{bmatrix}, \\ [G] &= \begin{bmatrix} 1 & 1 & \cdots & 1 \\ g_1(x_1, y_1) & g_1(x_2, y_2) & \cdots & g_1(x_N, y_N) \\ \vdots & \vdots & \ddots & \vdots \\ g_N(x_1, y_1) & g_N(x_2, y_2) & \cdots & g_N(x_N, y_N) \end{bmatrix} \\ [G_x] &= \begin{bmatrix} 0 & 0 & \cdots & 0 \\ g_x^n(1,1) & g_x^n(1,2) & \cdots & g_x^n(1,N) \\ \vdots & \vdots & \ddots & \vdots \\ g_x^n(N,1) & g_x^n(N,2) & \cdots & g_x^n(N,N) \end{bmatrix} \end{aligned}$$

The elements of matrix $[G]$ are given by equation (4). For matrix $[G_x]$, we can successively differentiate equation (4) to get its elements. For example, the first order derivative of $g_j(x, y)$ with respect to x can be written as

$$\begin{aligned} \frac{\partial g_j(x, y)}{\partial x} &= \frac{x - x_j}{\sqrt{(x - x_j)^2 + (y - y_j)^2 + c_j^2}} \\ &- \frac{x - x_i}{\sqrt{(x - x_i)^2 + (y - y_i)^2 + c_i^2}} \end{aligned} \quad (6)$$

With the known matrices $[G]$ and $[G_x]$, the weighting coefficient matrix $[W^n]$ can be obtained by using a direct method of LU decomposition. The weighting coefficient matrix of the y -derivative can be obtained in a similar manner.

In the local MQ-DQ method, the shape parameter c has a strong influence on the accuracy of numerical results. The optimal value of c is mainly affected by the number of supporting knots and the size of supporting region. Usually, the number of supporting knots is fixed for an application. The size effect of supporting region can be removed by normalization of scale in the supporting domain. The idea is actually motivated from the finite element method, where each element is usually mapped into a regular shape in the computational space. The essence of this idea is to transform the local support region to a unit square for the two dimensional case. The normalization can be made by the following transformation

$$\bar{x} = \frac{x}{D_i}, \quad \bar{y} = \frac{y}{D_i} \quad (7)$$

where (x, y) represents the coordinates of supporting region in the physical space, (\bar{x}, \bar{y}) denotes the coordinates in the square, D_i is the side length of the minimal square enclosing all knots in the supporting region for the knot i . The corresponding MQ basis functions in the local support now become

$$\varphi = \sqrt{\left(\bar{x} - \frac{x_i}{D_i}\right)^2 + \left(\bar{y} - \frac{y_i}{D_i}\right)^2 + \bar{c}^2}, \quad i = 1, \dots, N, \quad (8)$$

Compared with the traditional MQ-RBF, we can find that the shape parameter c is actually equivalent to $\bar{c}D_i$. The coordinate transformation (7) also changes the formulation of the weighting coefficients in the local MQ-DQ approximation. For example, by using the differential chain rule, the first order partial derivative with respect to x can be written as

$$\frac{\partial f}{\partial x} = \frac{\partial f}{\partial \bar{x}} \frac{d\bar{x}}{dx} = \frac{1}{D_i} \frac{\partial f}{\partial \bar{x}} = \frac{1}{D_i} \sum_{j=1}^N w_{i,j}^{(1)} f_j = \sum_{j=1}^N \frac{w_{i,j}^{(1)}}{D_i} f_j \quad (9)$$

where $w_{i,j}^{(1)}$ are the weighting coefficients computed in the unit square, $w_{i,j}^{(1)}/D_i$ are the actual weighting coefficients in the physical domain. Clearly, when D_i is changed, the equivalent c in the physical space is automatically changed. In our application, \bar{c} is chosen as a constant. Its optimal value depends on the number of supporting knots. In this study, the number of knots in the supporting region of the interior nodes is fixed as 17, which is considered to be able to give high order of accuracy from our experiences. The free shape parameter \bar{c}^2 is taken as 3.1, according to the previous work of [Shu, Ding, and Yeo (2003)].

3 Computation of Incompressible Navier-Stokes Equations by Local MQ-DQ Method

The two dimensional Navier-Stokes equations in the vorticity-stream function form are solved to evaluate the accuracy and reliability of local MQ-DQ method. The governing equations can be written as

$$\frac{\partial^2 \psi}{\partial x^2} + \frac{\partial^2 \psi}{\partial y^2} = \omega \quad (10)$$

$$\frac{\partial \omega}{\partial t} + u \frac{\partial \omega}{\partial x} + v \frac{\partial \omega}{\partial y} = \frac{1}{Re} \left(\frac{\partial^2 \omega}{\partial x^2} + \frac{\partial^2 \omega}{\partial y^2} \right) \quad (11)$$

where u, v denote the components of velocity in the x and y direction, which can be calculated from the stream function

$$u = \frac{\partial \psi}{\partial y}, \quad v = -\frac{\partial \psi}{\partial x} \quad (12)$$

Re is the Reynolds number. Similar to the conventional FD scheme, equations (10), (11) can be easily discretized by the local MQ-DQ method. In this work, the resultant algebraic equations are solved by SOR iteration method if steady flow is considered. For the unsteady flow, an explicit four-stage Runge-Kutta scheme is used to advance the vorticity solution in the time domain.

4 Applications and Discussion

Three test problems are considered in this work. The first case is the driven flow in a square cavity, which is a steady flow problem. The second case is the flow around a circular cylinder, which demonstrates an unsteady periodic flow pattern when the Reynolds number exceeds the critical value ($Re \approx 49$). The third case is the flow around two cylinders in the staggered arrangement, which is a much more complicated case. That is because a dynamic interaction between the shed vortices, shear layers and Karman vortex streets appears in the wake behind the cylinders. These cases are used to explore the applicability, robustness and advantages of local MQ-DQ method for simulation of incompressible viscous flows.

4.1 Driven Cavity Flow

We have conducted the computation for various Reynolds numbers for the lid-driven flow in a square cavity, and compared the present results with those of [Ghia,

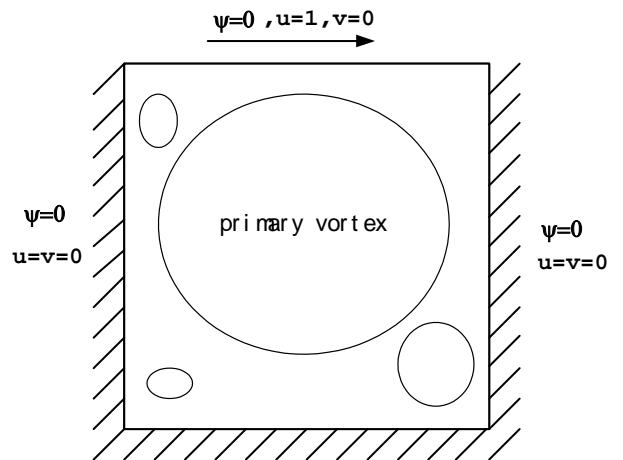


Figure 1 : Lid-driven flow in a square cavity

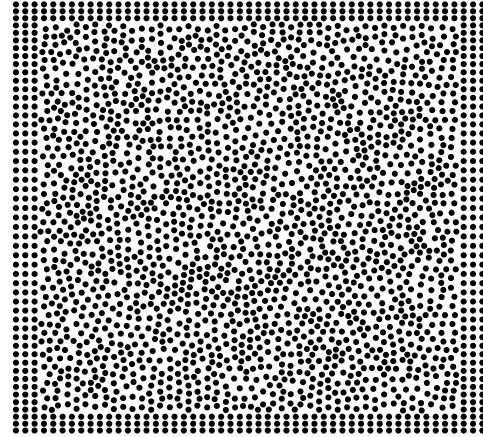
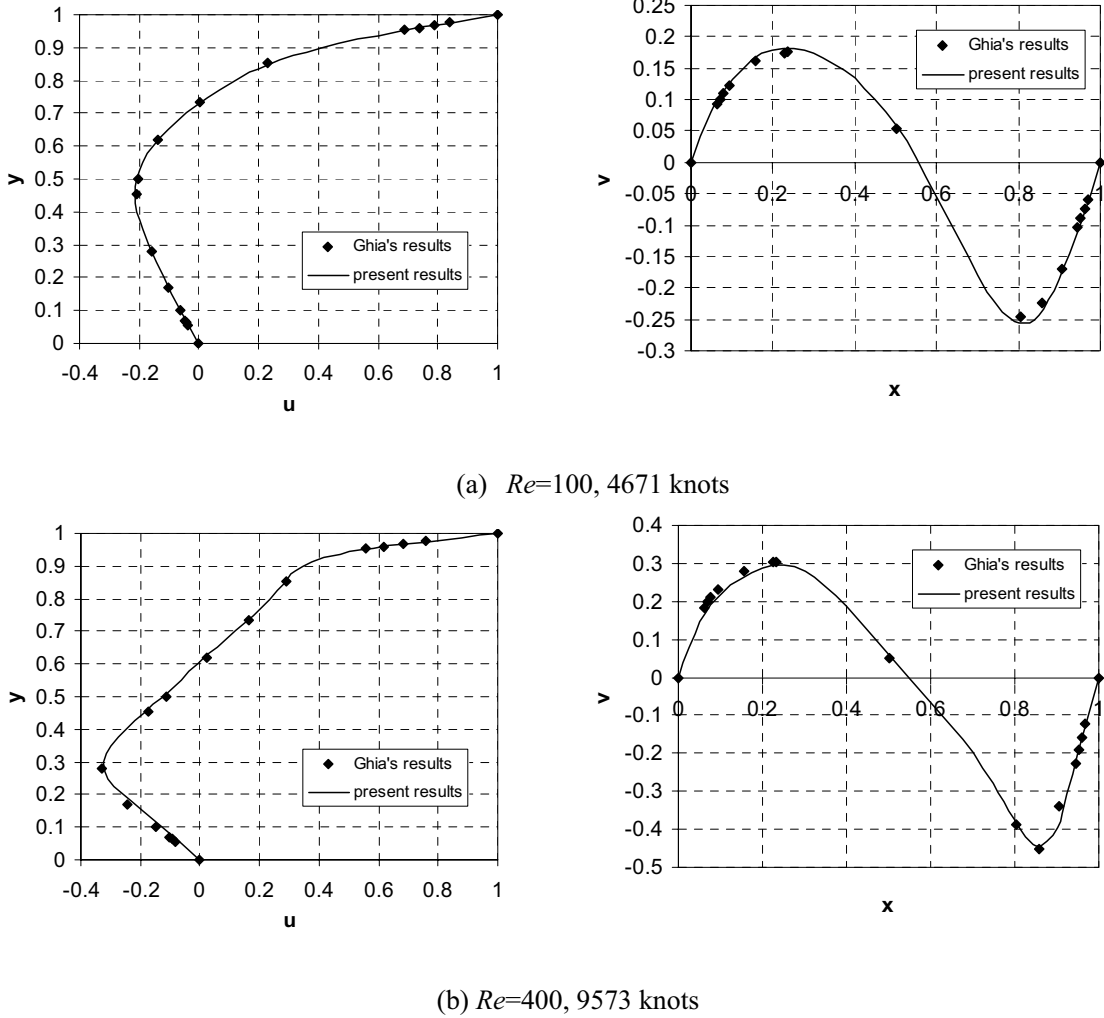


Figure 2 : Orthogonal boundary grids and interior random knots

Ghia, and Shin (1982)], which are considered as benchmark data in the literature. The configuration of this case is shown in Fig. 1. The boundary condition for the stream function can be easily implemented, i.e., $\psi_{boundary} = 0$, corresponding to Dirichlet condition. For this problem, the updating of vorticity on the wall involves the derivatives of stream function. Like the governing equations, these derivatives can also be discretized by the local MQ-DQ method. They can also be approximated by the conventional one-sided second order FD scheme. Two types of discretization are employed: one uses 4671 nodes and the other uses 9573 nodes. The former discretization is applied for the flow simulation with Reynolds number $Re=100$, and the latter one for the flow simulations



with $Re=400$, 1000 and 5000. Here, Reynolds number is defined as $Re = \frac{U_{lid}L}{\nu}$, where U_{lid} denotes the lid velocity, L denotes the length of the square side, and ν denotes the kinematic viscosity. A typical nodal distribution is shown in Fig. 2. As discussed in [Shu, Ding, and Yeo (2003)], the locally orthogonal grids near the boundaries are used to simplify the implementation of vorticity boundary condition.

It was found that the agreement between present numerical results and those from [Ghia, Ghia, and Shin (1982)] is very good. This can be observed in Fig. 3, which shows the velocity profiles through the center of cavity. Note that in general the present results are obtained by using less knots than those used in Ghia's computations.

4.2 Flow Around A Circular Cylinder

It is well-known that the cylinder flow demonstrates a periodically unsteady pattern when the Reynolds number is larger than the critical value ($Re_{critical} \approx 49$). Since this problem has been studied by many researchers, it is often used to examine the performance of new numerical methods in the unsteady flow simulation. In this work, we conducted the computation for the flow around a circular cylinder with Reynolds numbers of $Re=100$ and 200. Here, $Re = \frac{U_\infty D}{\nu}$, U_∞ is the free-stream velocity, D is the cylinder diameter, and ν is the kinematic viscosity.

The configuration of this problem is illustrated in Fig. 4. The in-flow velocity is specified with a free stream velocity U_∞ , which is equivalent to impose the boundary condition for stream function with $\psi = U_\infty \cdot y$ and vorticity with $\omega = 0$. The top and bottom boundaries are located

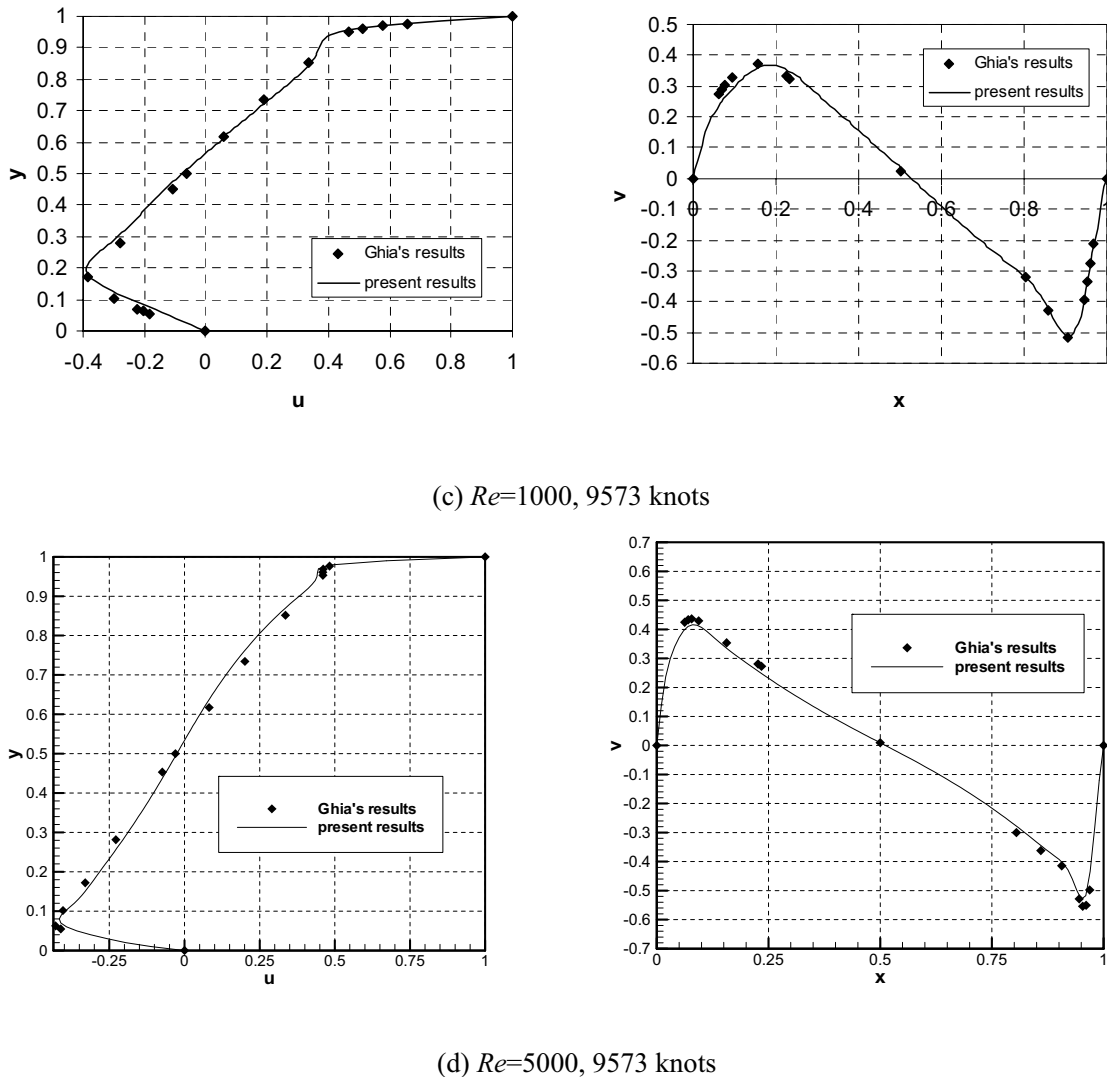


Figure 3 : U (left) and V (right) velocity profiles along vertical and horizontal central lines

at a transversal distance of 16 times of the cylinder diameter, which is assumed far enough to be the far-field according to literature [Behr, Hastreiter, Mittal, and Tezduyar (1995)]. The boundary condition imposed at these places is the same as the in-flow boundary. The out-flow boundary is located at a distance of 30 times of the cylinder diameter downstream of the rear of the cylinder. It is known that in the multiply-connected domain, the value of stream function at the surface of stationary body is an unknown constant, and this unknown constant may vary with time. To determine this unknown constant, the single-pressure condition is implemented according to literature [Tezduyar, Glowinski, and Liou (1988)]. In this test case, a total of 17463 nodes have been used with

a minimum “grid size” of 0.013. The time step is set to 0.01. The node distribution can be seen in Fig. 5. This set of nodes is generated by truncating a polar mesh.

Again, the present results agree very well with available data in the literature. The drag, lift coefficients and Strouhal number are shown in Table 1, and compared with results from [Liu, Zheng, and Sung (1998)], which shows a very good agreement. Figs. 6 & 7 present the streamlines and vorticity contours for unsteady cases of $Re=100$ and 200. The streamlines indicate the flow pattern at a given instant of time, and the vorticity contours illustrate the instantaneous vortex structure in the wake region.

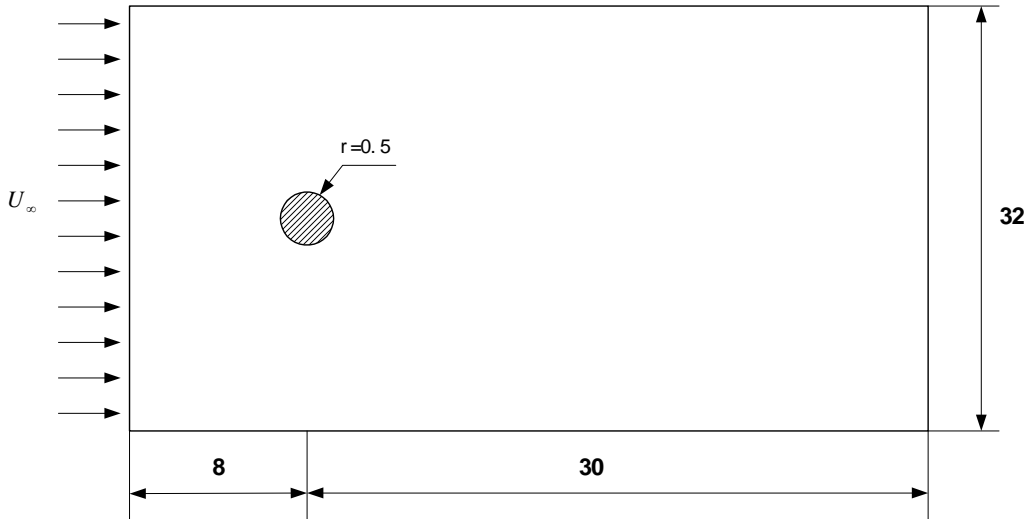


Figure 4 : Configuration of flow around one isolated cylinder

Table 1 : Comparison of drag and lift coefficients for $Re = 100$ and 200

Numerical results	Drag (C_d)		Lift (C_l)		Strouhal number (St)	
	$Re=100$	$Re=200$	$Re=100$	$Re=200$	$Re=100$	$Re=200$
Liu, Zheng, and Sung (1998)	1.350 ± 0.012	1.31 ± 0.049	± 0.339	± 0.69	0.164	0.192
Present	1.362 ± 0.010	1.352 ± 0.049	± 0.32	± 0.62	0.166	0.192

4.3 Flow Around A Pair of Staggered Cylinders

The third test case is the flow around a pair of staggered cylinders. The configuration of this problem is illustrated in Fig. 8. This case has been developed to test the behavior of the scheme on a cloud of knots generated by a simple node generator. Since local RBF-DQ method is a truly mesh-free method, it only requires node generation instead of mesh generation. Therefore, the computational cost should be relatively lower than traditional mesh generator in the sense of human labor and computational efforts. More precisely, it is at least true for this case. From the viewpoint of traditional mesh-based methods such as finite difference (FD) and finite element (FE), to simulate the flow around a pair of staggered cylinders, they have to either use a mesh generator to produce unstructured meshes or generate body-fitting meshes by coordinate transformation. Despite of the expensive computa-

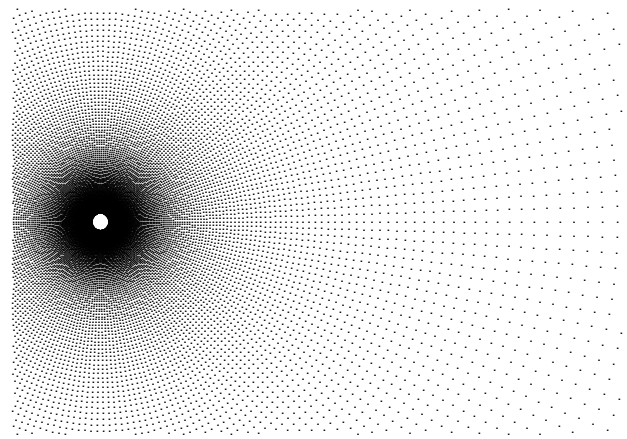


Figure 5 : Node distribution for flow past one isolated circular cylinder

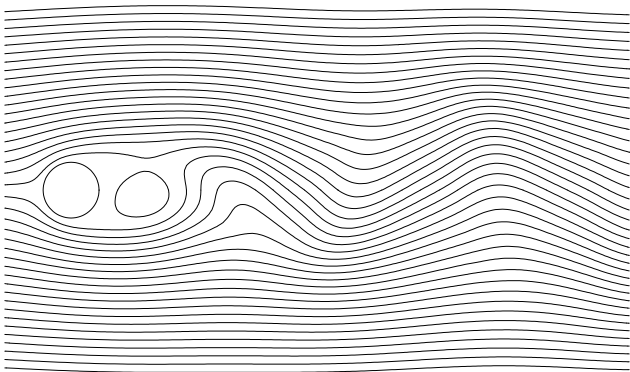


Figure 6 : Streamlines and vorticity contours for $Re = 100$

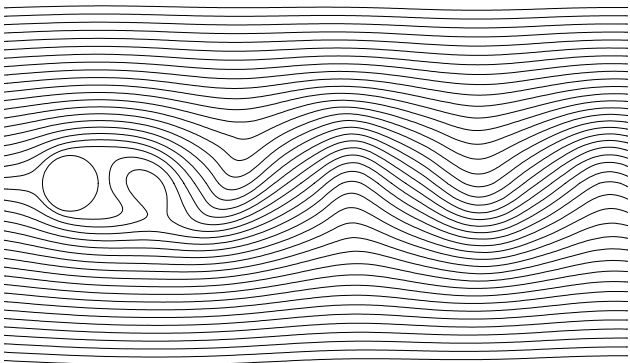


Figure 7 : Streamlines and vorticity contours for $Re = 200$

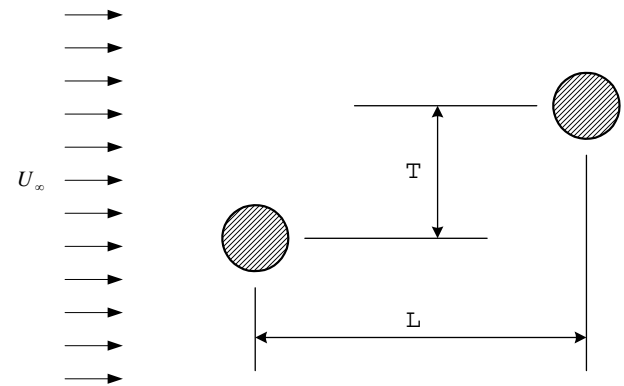


Figure 8 : Geometrical description of flow past a pair of cylinders

tional costs, the quality of generated mesh still needs interactive communications between the computer and the end-user to make sure that an appropriate mesh is produced. However, as shown in Fig. 9, the node generator for this case can be designed in a very simple manner. It is equivalent to a combination of two truncated polar grids. This way of node generation is not only simple, but also able to easily control the variation of nodal density in order to save computational costs.

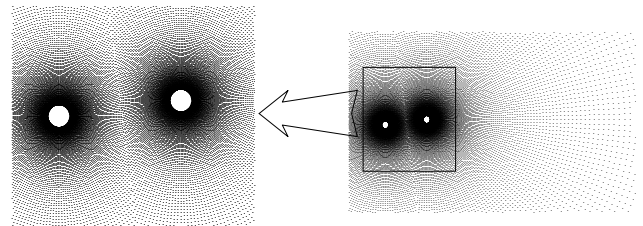
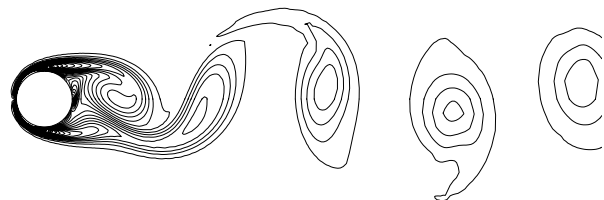


Figure 9 : Node distribution for the flow around two staggered circular cylinders



In the present investigation, the two staggered cylinders were arranged with streamwise gap of $L = 5.5D$ and transverse gap of $T = 0.7D$. The implementation of initial and boundary conditions are the same as those in the cases for flow around one isolated circular cylinder. The definition of Reynolds number is also based on the diameter of cylinder. In this study, a total of 43079 nodes was used with a minimum “grid size” of 0.013. The node distribution is depicted in Fig 9. The time step is set to 0.01, which is the same as in the case for one isolated cylinder. Instantaneous vorticity contours are shown in Fig. 10 for

the flow field visualization at $Re = 100$ in one complete circle. It can be seen that a Karman street is formed behind the upstream cylinder, and shed. It is clear that vortex shedding from the downstream cylinder is highly disturbed by the impingement of the upstream vortex street. Quantitative evaluation of the impingement effect can be viewed from the temporal histories of drag and lift coefficients, which are shown in Figs. 11(a) and 11(b). It can be seen that the lift coefficients of the upstream and downstream cylinders vary synchronizingly, which implies the synchronization between the impingement flow and vortex shedding from the downstream cylinder. The effect of staggered arrangement can be observed in the histories of drag coefficients. The drag coefficients of both cylinders can not maintain a *SINE* function, which is the case for one isolated cylinder. The mean values of drag coefficients are 1.306 and 0.790 for the upstream and downstream cylinders, respectively. Due to the synchronization, the upstream and downstream cylinders have the same Strouhal number of 0.156.

The successful simulation of the complex flow phenomenon around two circular cylinders in the staggered arrangement demonstrates the robustness and flexibility of present local MQ-DQ method. It should be emphasized that a total of 43079 nodes have been used in this simulation. It is known that for the RBF-based schemes, the problem of ill-conditioned global matrix becomes more and more serious when the nodes increase. It is almost impossible to employ very large number of nodes to solve a practical problem without very careful preconditioning. However, from the simulation of flow around two staggered cylinders, these problems are completely avoided in our simulation.

5 Conclusion

The recently developed local MQ-DQ method has been applied in this work to solve two-dimensional incompressible Navier-Stokes equations. Three test cases, which involve steady flow and unsteady flow with geometrical and dynamic complexity, are considered in this paper. The agreement between the obtained results and benchmark solution indicates that the present method can achieve very good performance in the simulation of two-dimensional incompressible flows. The accurate capture of complex phenomenon in the flow past two staggered cylinders demonstrates the ability of the method in the flow simulation with geometrical and dynamic complex-

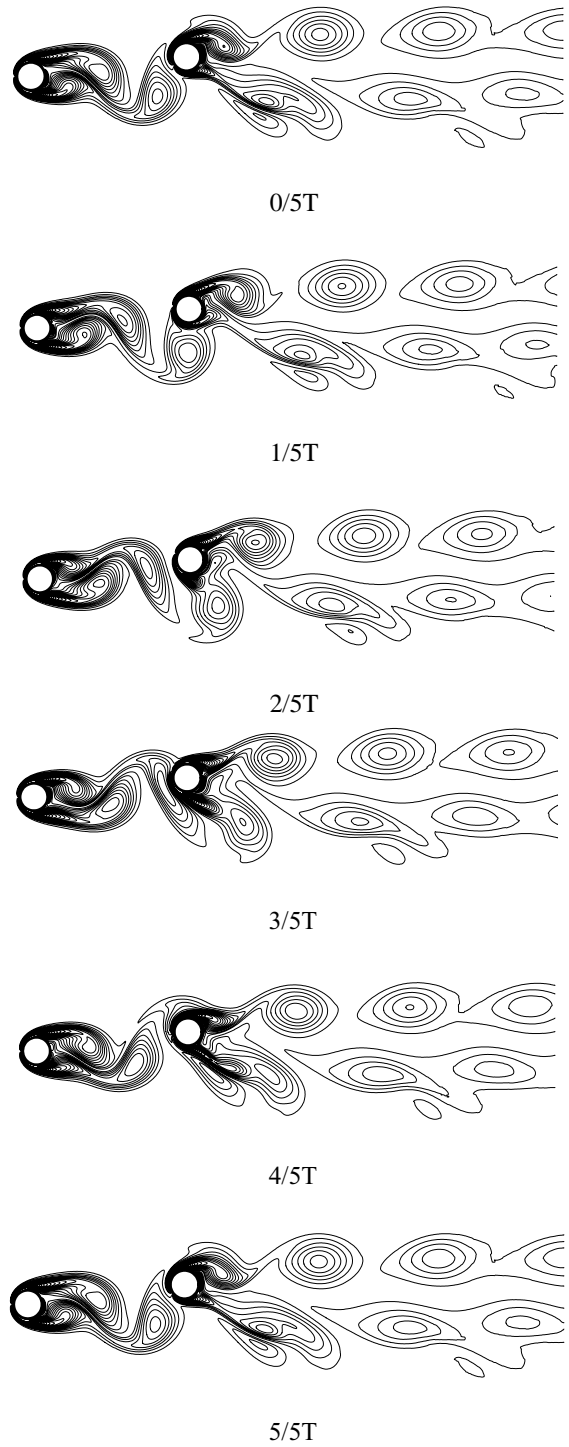


Figure 10 : Vorticity contours for the flow around two staggered circular cylinders at $Re = 100$ in one complete circle

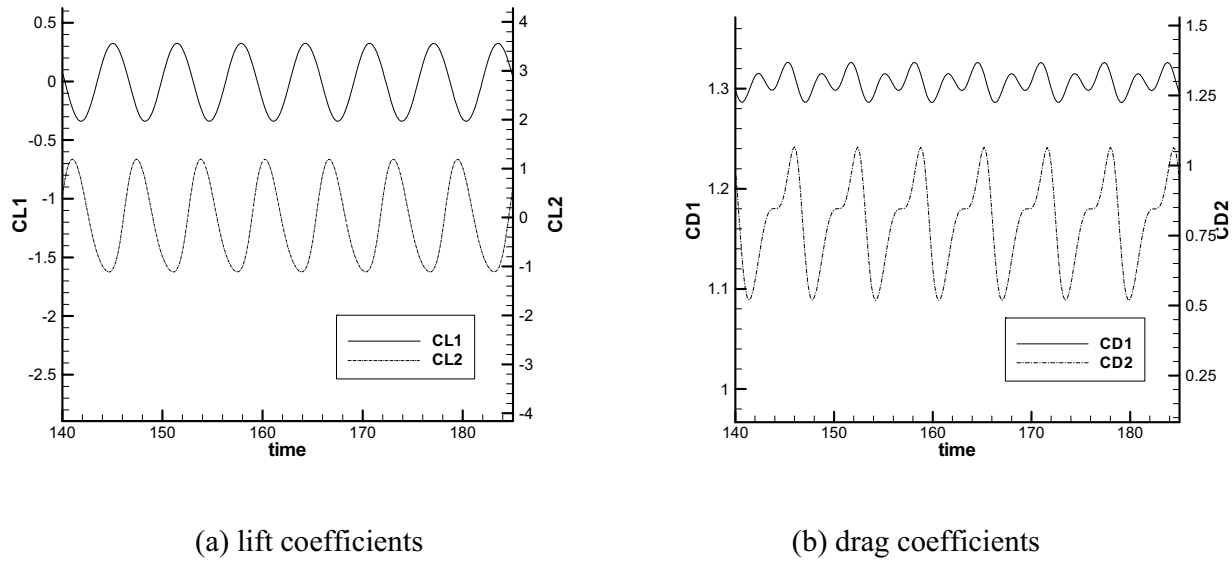


Figure 11 : Time history of drag and lift coefficients for the flow around two staggered circular cylinders at $Re = 100$

ity.

Overall, we believe that the simplicity and flexibility of the local MQ-DQ method could be extensively applied in the solution of partial differential equations on an irregular domain.

References

- Atluri, S. N.** (2004): The Meshless Method(MLPG) for Domain & BIE Discretizations. *Tech Science Press*, 700 pages.
- Atluri, S. N.; Han, Z. D.; Rajendran, A. M.** (2004): A New Implementation of the Meshless Finite Volume Method, Through the MLPG “Mixed” Approach, *CMES: Computer Modeling in Engineering & Sciences*, Vol. 6, No. 6, pp. 491-514.
- Atluri, S. N.; Shengping, S.** (2002): The Meshless Local Petrov-Galerkin (MLPG) Method: A Simple \& Less-costly Alternative to the Finite Element and Boundary Element Methods, *CMES: Computer Modeling in Engineering & Sciences*, Vol. 3, No. 1, pp. 11-52.
- Behr, M.; Hastreiter, D.; Mittal, S.; Tezduyar, T. E.** (1995): Incompressible flow past a circular cylinder: dependence of the computed flow field on the location of the lateral boundaries. *Comput. Methods Appl. Mech. Engrg.* Vol. 123, pp. 309-316.
- Bellman, R. E.; Kashef, B. G.; Casti, J.** (1972): Differential quadrature: A technique for the rapid solution of nonlinear partial differential equations. *J. Comput. Phys.* Vol. 10, 40-52.
- Chen, C. S.; Brebbia, C. A.; Power, H.** (1998): Dual reciprocity method using for Helmholtz-type operators. *Boundary Elements*, Vol. 20, pp. 495-504.
- Chen, W.; Tanaka, M.** (2002): A meshless, integration-free, and boundary-only RBF technique. *Comput. Math. Appl.*, Vol. 43, pp. 379-391.
- Fasshauer, G. E.** (1997): Solving partial differential equations by collocation with radial basis functions. *Surface fitting and multiresolution methods*, eds. A. L. Mahaute, C. Rabut and L. L. Schumaker, pp. 131-138.
- Forberg, B.; Driscoll, T. A.** (2002): Interpolation in the limit of increasingly flat radial basis functions. *Comput. Math. Appl.*, Vol. 43, pp. 413-422.
- Ghia, U.; Ghia, K. N.; Shin, C. T.** (1982): High-Re solutions for incompressible flow using the Navier-Stokes equations and a multi-grid method. *Journal of computational physics*, Vol. 48, pp. 387-411.
- Hon, Y. C.; Wu, Z. M.** (2000): A quasi-interpolation method for solving stiff ordinary differential equations. *International Journal for Numerical Methods in Engineering*, Vol. 48, pp. 1187-1197.
- Kansa, E. J.** (1990): Multiquadratics – A scattered data approximation scheme with applications to computational fluid-dynamics –I. Surface approximations and partial derivative estimates. *Computers Mathematics ap-*

plication, Vol. 19, No (6-8) pp. 127-145.

Lin, H.; Atluri, S. N. (2001): The Meshless Local Petrov-Galerkin (MLPG) Method for Solving Incompressible Navier-Stokes Equations, *CMES: Computer Modeling in Engineering & Sciences* Vol. 2, No. 2, pp. 117-142.

Liu, C.; Zheng, X.; Sung, C. H. (1998): Preconditioned multigrid methods for unsteady incompressible flows. *J. Comput. Phys.* 139, 35.

Mai-Duy, N.; Tran-Cong, T. (2001a): Numerical solution of differential equations using multiquadric radial basis function networks. *Neural Networks*, Vol. 14, pp. 185-199.

Mai-Duy, N.; Tran-Cong, T. (2001b): Numerical solution of Navier-Stokes equations using radial basis function networks. *Int. J. Numer. Meth. Fluids*, Vol. 37, pp. 65-86.

Richards, B. E.; Shu, C. (1992): Application of generalized differential quadrature to solve two-dimensional incompressible Navier-Stokes equations. *Int. J. Numer. Methods Fluids*. 15, 791-798.

Shu, C. (2000): Differential Quadrature and its Application in Engineering, Springer-Verlag London Limited.

Shu, C.; Ding, H.; Yeo, K. S. (2003): Local radial basis function-based differential quadrature method and its application to solve two-dimensional incompressible Navier-Stokes equations. *Comput. Methods Appl. Mech. Engrg.* Vol. 192, pp. 941-954.

Tezduyar, T. E.; Glowinski, R.; Liou, J. (1988): Petrov-Galerkin methods on multiply connected domains for the vorticity-stream function formulation of the incompressible Navier-Stokes equations. *Int. J. numer. Methods fluids*, Vol. 8, pp. 1269-1290.

Tolstykh; Shirobokov (2003): On using radial basis functions in a ‘finite difference mode’ with applications to elasticity problems. *Computational Mechanics*, Vol. 33, pp. 68- 79.

Wu, Y. L.; Shu, C. (2002): Development of RBF-DQ Method for Derivative Approximation and Its Application to Simulate Natural Convection in Concentric Annuli. *Computational Mechanics*, Vol. 29, pp. 477-485.

